Modified asymptotic approach to modeling a dilute-binary-alloy solidification front

James M. Hyman
Center for Nonlinear Studies, Theoretical Division, MS B284, Los Alamos National Laboratory, Los Alamos, New Mexico 87545

Amy Novick-Cohen
Department of Mathematics, Michigan State University, East Lansing, Michigan 48824

Philip Rosenau
Department of Mechanical Engineering, Technion, Israel Institute of Technology, Haifa 32000, Israel
(Received 19 June 1987)

Directional solidification in the presence of an impurity may be described by a set of impurity-concentration and thermal-diffusion equations coupled at a free boundary. Small deviations of the interface from planarity can be described by a single fourth-order equation. This equation is derived by a long-wavelength, small-amplitude expansion in the limit of a small distribution coefficient. We present an alternative asymptotic approach that isolates and preserves the crucially important nonlinearities in their original form, and thus preserves the proper behavior at large amplitudes during pattern formation. The resulting evolution equation is in better agreement with the physical phenomena of front destabilization and droplet creation than are previously presented models. The formation of different solidification patterns is numerically elucidated.

I. INTRODUCTION AND STATEMENT OF THE PROBLEM

The solidification front of a dilute binary alloy is sensitive to the delicate balance between competing nonlinear processes. In deriving equations that describe the evolution of the front, it is essential to properly preserve these nonlinearities. The amplitude equation derived using standard asymptotic methods, such as in Ref. 1, predicts the solution to blow up within a finite time. Generally speaking, the exact form and nature of the blowup—and in fact, whether or not the solution blows up at all—can be highly dependent on how the nonlinearities are approximated by the asymptotic expansion.

To better model the interface, rather than go to a more complex physical model, we developed a refined derivation that preserves the crucial nonlinearities of the full equations and thus overcomes the major difficulty of Ref. 1. The derivation will be outlined in Sec. II, followed by numerical studies in Sec. III and a discussion of the results in Sec. IV. We now give a brief description of the solidification problem.

Directional solidification is a process in which an alloy is transported with a fixed velocity V through an externally imposed temperature gradient. This process has many metallurgical applications, including zone refinement. Repeated directional solidification of a dilute binary alloy (the minor phase here is the impurity) gradually reduces the amount of impurity in the alloy. This occurs primarily because K, the segregation coefficient (defined as the ratio of the impurity concentration on the solid side to the impurity concentration on the liquid side of a planar solid-liquid interface at thermodynamic equilibrium), is frequently much less than 1.

Written in terms of the moving coordinate frame $\hat{\mathbf{z}} \equiv \hat{\mathbf{z}}_{\text{old}} - V\hat{\mathbf{t}}$, and using the diffusion coefficient D of the impurity in the solute to nondimensionalize the problem, the equations for the impurity concentration and the temperature profiles in terms of the spatial variables $(x,y,z)=(D/V)(\hat{\mathbf{x}},\hat{\mathbf{y}},\hat{\mathbf{z}})$ and the time variable $t=DV^{-2}\hat{\mathbf{t}}$ are (Refs. 2–4)

$$\Delta C + C_z - C_t = 0, \quad z > \psi \tag{1a}$$

$$\Delta T = 0, \quad z > \psi \tag{1b}$$

$$\Delta \tilde{T} = 0, \quad z < \psi \, . \tag{1c}$$

On the surface $z=\psi(\mathbf{x},t)$ we also have the conditions

$$T = 1 + MC + \gamma\kappa = \tilde{T} \, , \tag{1d}$$

$$R(\mathbf{n}\cdot\nabla T) - (\mathbf{n}\cdot\nabla T) = FV_n \, , \tag{1e}$$

$$\mathbf{n}\cdot\nabla C = (K-1)CV_n \, , \tag{1f}$$

where κ is the curvature, $\mathbf{n}$ is the unit vector normal to the interface, and V_n is the normal component of the velocity of the interface. Here $\psi(\mathbf{x},t)$ denotes the location of the liquid-solid interface, which will be assumed here to be sharp. The liquid (solid) side of the interface will be located at $z > \psi$ ($z < \psi$). The concentration of the impurity $C(\mathbf{x},t)$ has been normalized to be unity at the liquid side of the interface. The temperature $T(\mathbf{x},t)$ [$\tilde{T}(\mathbf{x},t)$], at the liquid (solid) side of the interface has been normalized so that the melting temperature at a planar interface with no impurity will be unity.

Here $M = mC^*/T_M$ is the slope of the liquidus line on the phase diagram, T_M is the melting temperature (in kelvin) of the pure solvent, and C^* is the solvent concentration in the liquid at the interface when the interface is

planar. If we limit ourselves to supersaturated solutions, then we may assume that m (and hence, M) is negative. Also, $\gamma=\Gamma V/D$, where Γ is the capillary constant, and K_S (K_L) is the thermal conductivity of the solid (liquid), $F=DL/K_L T_M$, where L is the latent heat of fusion per unit volume, and $R=K_S/K_L$. In obtaining Eqs. (1a)–(1f), we have assumed that the thermal diffusivities, D_S and D_L, are much larger than the diffusion coefficient of the solution.[2]

Note that Eqs. (1) admit the following stationary planar interface:

$$T^e=1+M+Gz\ , \tag{2a}$$

$$\tilde{T}^e=1+M+Gz/R\ , \tag{2b}$$

$$C^e=K+(1-K)e^{-z}\ , \tag{2c}$$

where G is arbitrary and corresponds to the slope of an externally imposed temperature profile. We will assume that far from the interface the temperature and concentration profiles are not influenced by the deviations of the interface from planarity. Hence, we impose the far field conditions

$$C(x,t)\to C^e(z),\quad T(x,t)\to T^e(z),\quad z\to\infty \tag{2d}$$

$$\tilde{T}(x,t)\to\tilde{T}^e(z),\quad z\to-\infty\ . \tag{2e}$$

In assuming this set of equations to model the behavior of a dilute binary alloy, we have neglected the coupling of these equations to an underlying hydrodynamic field. Likewise, we have neglected the possibility of deviations from local thermal equilibrium along the solidification front as well as the possibility of nonisotropic attachment kinetics. These other effects have recently been taken into account elsewhere.[5–7] Our goal here is to study a simple system that is nevertheless capable of conveying the crucial features of a typical solidification front. For the richness of phenomena contained in this set of equations see, for example, the numerical calculations of Brown[8–11] *et al.*

If the solid-liquid interface is planar during directional solidification, even if impurities still remain in the resulting solid, these impurities will be uniformly distributed. If the interface deviates strongly from planarity, then the resulting solid may contain bands of impurity zones. These impurity striations may reduce the strength or otherwise alter the properties of the resulting solid. Thus, in applications, it is important to be able to control and understand the behavior of the solid-liquid interface, $\psi(\mathbf{x},t)$.

Several authors (Refs. 1, 5–7, 12, and 13) have used asymptotic methods to derive a single evolution equation for $\phi(x,t)=\psi(\mathbf{x},t)/\epsilon$ from the full set of Eqs. (1)

$$\phi_t=(-\phi+\tfrac{1}{2}\phi^2)_{xx}-\beta\phi_{xxxx}-K\phi\ . \tag{3}$$

Here ϵ is a dimensionless scaling parameter. The basis for these derivations has been the isolation of certain parameter regimes where the long-wavelength instability dominates and enables an effective separation of scales. This occurs when the deviations vary slower in the direction parallel to the interface than in the direction normal to the interface. In particular, such a separation of scales is possible if $K\ll 1$ and if $L\ll 1$ (Refs. 1 and 12).

The solutions of Eq. (3) apparently either decay to zero or blow up in finite time. Neither behavior approximates well or corresponds closely with the patterns that have been observed experimentally and numerically [within the context of the full set of Eqs. (1a)–(1f)]. It is the inadequacy of Eq. (3) to describe the phenomena contained in the equations from which it was derived that motivated us to look for an alternative asymptotic approach, which will be described next.

II. DERIVATION

Our goal is to isolate and maintain the underlying nonlinearities that are crucial to the asymptotic evolution in our equation. The boundary condition (1d) is a nonlinear function of the curvature. If the boundary condition in Eqs. (1e) and (1f) are multiplied by the metric, they contain only polynomial nonlinearities. These boundary conditions are prescribed at a free interface, which is general is also nonlinear. It is possible to highlight this source of nonlinearity by employing curvilinear coordinates to "flatten out" the interface.

Similarly, to Ref. 1 we make the following simplifying assumptions: (1) the system is two dimensional, $\partial/\partial y\equiv 0$, the interface is single valued as a function of x, and $\psi=\psi(x,t)$; and (2) $F=0$ and $R=1$. (Succinonitrile should satisfy this last assumption.)[14] The last simplification has the advantage that the stationary planar solutions Eqs. (2b) and (2c) satisfy Eqs. (1a)–(1f) and Eqs. (2d) and (2e), irrespective of the location of the interface. This enables us to solve the remainder of the equations for $C(x,z,t)$ with the temperature profiles given by their stationary planar forms.

Under these assumptions, $C(x,z,t)$ satisfies

$$\Delta C+C_z-C_t=0,\quad z>\psi \tag{4a}$$

$$1=g\phi+C-\beta\kappa,\quad z=\psi \tag{4b}$$

$$\mathbf{n}\cdot\nabla C=(K-1)CV_n,\quad z=\psi \tag{4c}$$

$$C\to C^e(z),\quad z\to\infty\ , \tag{4d}$$

where $g=-G/M$ and $\beta=-\gamma/M$, and where $C^e(z)$ represents the planar profile [see Eq. (2)]. In terms of curvilinear coordinates, Eqs. (4a) and (4c) become $[z\to z-\psi(x,t)]$

$$C_{xx}+(1+\psi_x^2)C_{zz}-\psi_{xx}C_z-2\psi_x C_{xz}+C_z-C_t+\psi_t C_z=0,\quad z>0 \tag{5a}$$

$$\mathbf{n}\cdot\nabla C+\frac{\psi_x^2}{(1+\psi_x^2)^{1/2}}C_z=(K-1)CV_n,\quad z=0\ . \tag{5b}$$

Noting that

$$\mathbf{n}=\left[\frac{-\psi_x}{(1+\psi_x^2)^{1/2}},\frac{1}{(1+\psi_x^2)^{1/2}}\right] \text{ and } V_n=\frac{1+\psi_t}{(1+\psi_x^2)^{1/2}} ,$$

then rewriting Eqs. (5a) and (5b) in terms of $c=C-C^e(z)$ [where $C^e=K+(1-K)e^{-z-\psi}$] yields

$$c_{xx}+(1+\psi_x^2)c_{zz}+c_z(1-\psi_{xx}+\psi_t)-2\psi_x c_{xz}-c_t=0, \quad z>0 \tag{6a}$$

$$0=g\psi+c+(1-K)(e^{-\psi}-1)-\beta\kappa, \quad z=0 \tag{6b}$$

$$0=\psi_x c_x-(1-\psi_x^2)c_z+(K-1)c(1+\psi_t)+(K-1)(1-e^{-\psi})+(K-1)[K+(1-K)e^{-\psi}\mid\psi_t, \quad z=0 \tag{6c}$$

$$c\to 0, \quad z=\infty . \tag{6d}$$

All the nonlinearities in the above equations are clearly polynomial, except for $\exp(-\psi)$ and κ.

We now employ the scaling assumptions used in Ref. 1 and assume that

$$g=g_c(1-\epsilon), \quad K=\epsilon^2 K ,$$

$$\bar{x}=\epsilon^{1/2}x, \quad t=\epsilon^2 t, \quad \bar{z}=z .$$

This choice of scalings corresponds to the long-wavelength instability that occurs just below the limit of absolute stability.[1] We formally expand in ϵ,

$$c=c^{(0)}+\epsilon c^{(1)}+\epsilon^2 c^{(2)}+\cdots ,$$

$$\psi=\epsilon\psi^{(1)}+\epsilon^2\psi^{(2)}+\cdots ,$$

$$e^{-\psi}=F^{(0)}+\epsilon F^{(1)}+\epsilon^2 F^{(2)}\cdots ,$$

$$\kappa=\kappa^{(0)}+\epsilon\kappa^{(1)}+\epsilon^2\kappa^{(2)}\cdots .$$

Note that from the scaling assumptions on ψ and $\bar{x}$, it follows that $\kappa^{(0)}=\kappa^{(1)}=0$. At this point our approach deviates from the standard expansion in that we shall maintain the distinguishing $F^{(i)}-\kappa^{(i)}$ notation. This will allow us to later restore the original $e^{-\psi}$-κ dependence in the $O(\epsilon^3)$ evolution equation. This will be achieved by considering the highest-order terms $F^{(2)}$ and $\kappa^{(2)}$, not as third-order terms in an infinite expansion, but as a sum of the whole tail. For instance, $F^{(2)}$ will be defined as

$$F^{(2)}\equiv\epsilon^{-2}(e^{-\psi}-F^{(0)}-\epsilon F^{(1)}) . \tag{7}$$

In standard asymptotic expansion, a limiting, $\epsilon\to 0+$, operation is taken in Ref. 7 and eliminates higher-order terms. In this instance, it is the preservation of this tail that allows us to derive an expansion valid for large amplitudes.

In what follows, we drop the bar notation over the scaled variables. From the $O(1)$ equations, it follows that $c^{(0)}\equiv 0$.

The solution of the $O(\epsilon)$ equations,

$$c_{zz}^{(1)}+c_z^{(1)}=0, \quad z>0 \tag{8a}$$

$$g_c\psi^{(1)}+c^{(1)}+F^{(1)}=0, \quad z=0 , \tag{8b}$$

$$c_z^{(1)}+c^{(1)}=0, \quad z=0 \tag{8c}$$

$$c^{(1)}=0, \quad z=\infty \tag{8d}$$

yields

$$c^{(1)}=-(F^{(1)}+gc\psi^{(1)})e^{-z} .$$

The solution of the $O(\epsilon^2)$ equations,

$$c_{xx}^{(1)}+c_{zz}^{(2)}+c_z^{(2)}=0, \quad z>0 \tag{9a}$$

$$g_c\psi^{(2)}-g_c\psi^{(1)}+c^{(2)}+F^{(2)}-\beta\kappa^{(2)}=0, \quad z=0 , \tag{9b}$$

$$c_z^{(2)}+c^{(2)}=0, \quad z=0 \tag{9c}$$

$$c^{(2)}=0, \quad z=\infty \tag{9d}$$

yields

$$(F^{(1)}+g_c\psi^{(1)})_{xx}=0$$

and

$$c^{(2)}=(-F^{(2)}+\beta\kappa^{(2)}-g_c\psi^{(2)}+g_c\psi^{(1)})e^{-z} .$$

Requiring the solution to be bounded as $x\to\infty$ yields

$$F^{(1)}+g_c\psi^{(1)}=f(t) .$$

Without loss of generality, we may assume that $F^{(1)}=-\psi^{(1)}$, yielding $g_c=1$, $f(t)=0$, and $c^{(1)}\equiv 0$.

The solution of the $O(\epsilon^3)$ equations

$$c_{xx}^{(2)}+c_{zz}^{(3)}+c_z^{(3)}=0, \quad z>0 \tag{10a}$$

$$\psi^{(3)}-\psi^{(2)}+c^{(3)}+F^{(3)}-KF^{(1)}-\beta\kappa^{(3)}=0, \quad z=0 \tag{10b}$$

$$c_z^{(3)}+c^{(3)}-KF^{(1)}+\psi_t^{(1)}=0, \quad z=0 \tag{10c}$$

$$c^{(3)}=0, \quad z=\infty \tag{10d}$$

yields

$$c^{(3)}=(\psi^{(2)}-\psi^{(3)}+KF^{(1)}-F^{(3)}+\beta\kappa^{(3)})e^{-z}+(KF^{(1)}-\psi_t^{(1)})ze^{-z} , \tag{11}$$

and the evolution equation

$$0=\psi_t^{(0)}+(-F^{(2)}+\beta\kappa^{(2)}-\psi^{(2)}+\psi^{(1)})_{xx}-KF^{(1)} \tag{12}$$

as a consistency condition. Note that $\kappa^{(3)}$ does not appear in Eq. (12), neither is it needed at this level.

At this point we identify $F^{(0)}=1$, $F^{(1)}=-\psi^{(1)}$, and $\kappa^{(2)}=\kappa/\epsilon^2$. Thus, from Eq. (7) it follows that

$$F^{(2)}=(e^{-\psi}-1+\epsilon\psi^{(1)})/\epsilon^2 . \tag{13}$$

Finally, recalling that $\phi=\psi/\epsilon$ and rewriting Eq. (12) as

$$\phi_t = \epsilon^{-2}[e^{-\epsilon\phi} - 1 + (1-\epsilon)\epsilon\phi - \beta\kappa\,|_{xx} - K\phi + E\ , \qquad (14)$$

where

$$\kappa = \epsilon^2\phi_{xx}/(1+\epsilon^3\phi_x^2)^{3/2}$$

and E is a higher-order remainder,

$$E = -\epsilon(\psi_t^{(2)} + \psi_{xx}^{(2)} - K\psi^{(2)})\ ,$$

which henceforth will be ignored. Thus, the evolution of the interface is governed by

$$\phi_t = [\epsilon^{-2}(e^{-\epsilon\phi} - 1) + \epsilon^{-1}(1-\epsilon)\phi - \beta\phi_{xx}(1+\epsilon^3\phi_x^2)^{-3/2}]_{xx} - K\phi\ . \qquad (15)$$

When the bracketed term in Eq. (15) is expanded in small ϕ, it reduces to Eq. (3) to a leading order. However, for large amplitudes the behaviors of Eqs. (3) and (15) are very different. The new exponential term in Eq. (15) does not qualitatively change the solution's behavior. It is the term *due to surface tension* that introduces a meaningful change in the forming pattern. Indeed replacing the exponential by its leading approximation

$$\phi_t = [-\phi + \tfrac{1}{2}\phi^2 - \beta\phi_{xx}(1+\epsilon^3\phi_x^2)^{-3/2}]_{xx} - K\phi \qquad (16)$$

results in solutions with the same qualitative properties as Eq. (15). Thus, analytical studies of Eq. (16) can be used to gain insight into the properties of Eq. (15).

III. NUMERICAL STUDIES

We now present and summarize our numerical studies. Equations (3) and (15) were solved numerically on $[0,2\pi]$ with periodic boundary conditions. The spatial derivatives were approximated using the pseudo-spectral fast-fourier-transform (FFT) method and the equations were integrated in time using the backward differential formulas in the MOL1D package.[15] The number of spatial mesh points was varied between 128 and 512, and the time truncation error per unit step was varied between 10^{-6} and 10^{-10} to ensure the calculated solutions were sufficiently accurate.

The solutions in Figs. 1–4 show the time evolution of the initial data

$$\phi(x,0) = \lambda + \cos x, \quad -\infty < x < \infty\ . \qquad (17)$$

Figures 1(a) and 1(b) show the evolution for Eq. (3) with $\lambda = -10$. Note again that this solution is recovered from Eq. (14) as $\epsilon \to 0+$. Note also that as the blowup time (i.e., the time when the solution explodes) is approached, the main evolving pulse grows very fast and narrows down. This is evident in the change of scale from Eqs. (1a) and (1b) and further growth not shown here. The amplitude blowup in finite time can be derived through formal analysis[16] and was verified numerically by calculating the rate of blowup. A similar phenomenon is observed for the side lobes.

In Fig. 2, the evolution of the same initial data as in Fig. 1 is described, but for Eq. (15) with $\epsilon = 0.1$. Note that now the process comes to halt at almost one-third the time corresponding to Fig. 1. This appears to happen not because of the blowup of the interface, which appears

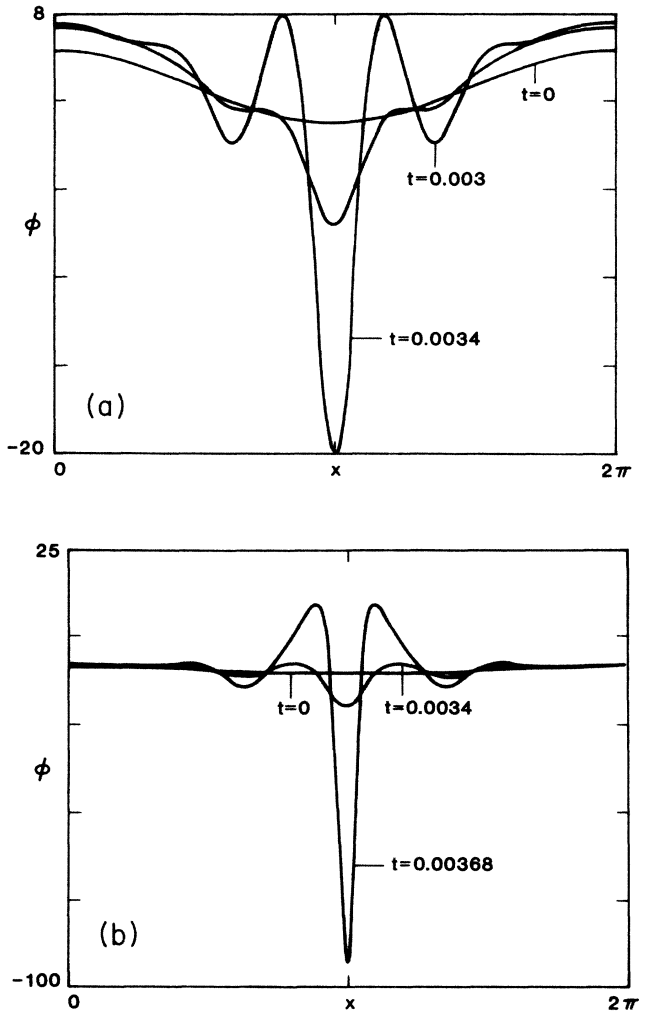

FIG. 1. (a) The solution of Eq. (3) with initial data $\phi(x,0) = -10 + \cos x$. (b) The evolution of the solution in (a) until later times. Note the change in scale.

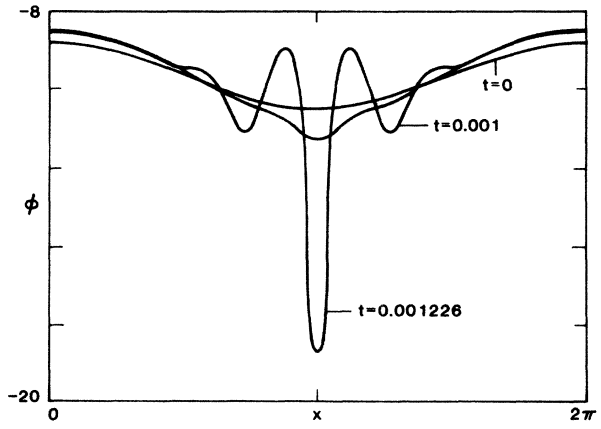

FIG. 2. The solution of Eq. (14) with $\epsilon = 0.1$ and $\phi(x,0) = -10 + \cos x$.

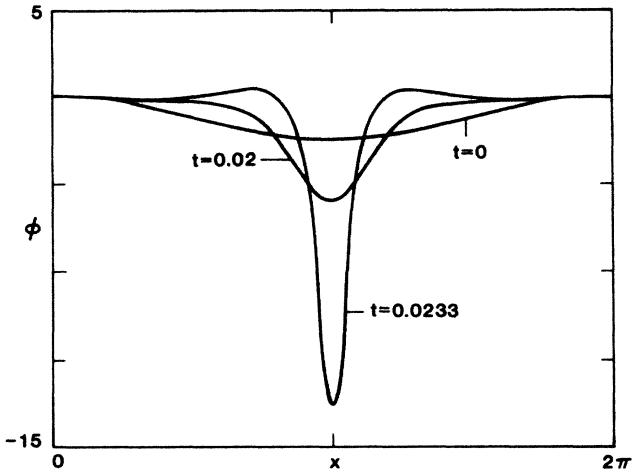

FIG. 3. The solution of Eq. (14) with $\epsilon=0.1$ and $\phi(x,0)=\cos x$.

to grow to a finite extent, but rather due to the steepening of the gradients at the sides of the forming finger. The number of side lobes is determined by the mean of the initial data, λ in Eq. (17). This mean determines the number of initially unstable (linear) eigenmodes. Therefore, for a given λ, both the regularized and unregularized equations will initially develop the same number of side lobes, even through the subsequent evolution is quite different.

In Fig. 3 we follow the finger formation for $\lambda=0$ and $\epsilon=0.1$. Note that the number of side lobes is reduced. Also, it takes longer for the side walls to become vertical and for the finger to saturate.

In Fig. 4 we return to $\lambda=-10$ but with $\epsilon=0.2$. Note that there is the same number of side lobes as in Figs. 1 and 2 but the finger develops much faster.

Thus, Eq. (15) removes the singular growth of the amplitude by a weaker singularity, an unbounded growth of its gradients. This leads to a halt in the amplitude

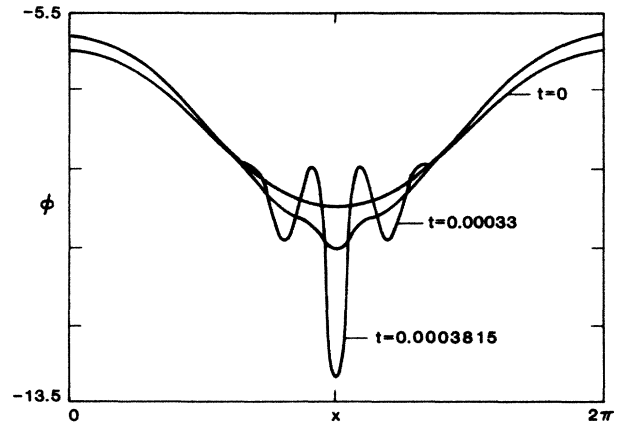

FIG. 4. The solution of Eq. (14) with $\epsilon=0.2$ and $\phi(x,0)=-10+\cos x$.

growth at a finite level. It is the unbounded growth of the gradients that makes the modification due to the tension far more important than the replacement of the quadratic term in Eq. (3) by an exponential one. Note also that close to the gradient's breakup, the main activity takes place at the tip of the finger. This is to be contrasted with the evolution of Eq. (3) shown in Fig. 1.

IV. CONCLUDING REMARKS

The inability of the amplitude Eq. (3) derived in Ref. 1 to model the observed physical phenomena may be interpreted as a sign that the basic physical model used is too simple to describe these physical phenomena. However, having clear numerical evidence[10,11] showing that this is not necessarily so, we opted to keep the model but to find a better asymptotic expansion to describe its dynamics.

The advance made in the present work is the realization that the conventional asymptotics, based on a small expansion amplitude, are inadequate to describe large amplitude deviation. By properly accounting for the nonpolynomial, nonlinear terms, we obtained an equation that does not collapse for large amplitudes. Generally, this goal may be achieved by replacing a Taylor-type series expansion by, say, an expansion in elementary or rational functions. The extra degree of freedom gained in this approach may be used to impose proper boundedness on the approximating solution at large amplitude. This idea was recently introduced in Ref. 17 and used in Ref. 18 where certain functions of operators describing the discrete vibration of a lattice were approximated by rational functions of operators. Thus, even if the solution is not expected to be of great precision at large amplitudes, the introduced regularizing procedure enables the dynamics to survive these high peaks of the solution.

Because of the relative simplicity of the present problem, we were able to retain the crucial nonlinearities that enter the problem in their original form and monitor their action at a given asymptotic level. Thus, while preserving the asymptotic expansion to a given order, we avoided a direct amplitude expansion of these nonlinearities. As a result, for small amplitude solutions, Eqs. (3a) and (15) are equivalent up to the third order; for large amplitude solutions, the nonlinearities (kept in their original form) provide the stabilizing mechanism.

In the numerical computations of Brown *et al.* (Ref. 10) on the full system of equations, verticality of the walls of the fingers of impurity was also quoted as being responsible for the breakdown of their approach. Notably, this difficulty still occurred when diffusion of the impurity in the solid was incorporated in their model. They concluded that the breakdown occurred because the requirement that the interface remain single-valued, $z=\phi(x,t)$, was overly restrictive.[11]

This type of breakdown also occurs in the closely connected droplet formation problem where the droplets cannot form at the tip of the fingers while the fingers are constrained to remain single-valued. Equation (15) follows the evolution of the interface up to the moment of

walls formation at which the breakdown of the gradients signals a loss of single valuedness. Up to this moment, Eq. (15) describes the evolution of the interface, but beyond it, a different approach (such as a parametric formulation) must be used.

The approach described here can also be applied to other problems where a direct amplitude expansion collapses. From this point of view, the present problem should be viewed as a pedagogical example.

ACKNOWLEDGMENTS

The authors thank David Levermore and Ann Stanley for useful discussions and remarks. This work was supported in part by the U.S. Department of Energy, under Contract No. W-7405-ENG-36, Applied Mathematical Sciences Research Program, KC-07-01-01, partially by Air Force Contracts Nos. AFOSR-85-0017 and AFOSR-86-0179.

[1]G. I. Sivashinsky, Physica (The Hague), **8D**, 243 (1983).
[2]D. J. Wollkind and L. A. Segel, Philos. Trans. R. Soc. London, Ser. A **268**, 351 (1970).
[3]W. W. Mullins and R. F. Sekerka, J. Appl. Phys. **34**, 323 (1963).
[4]W. W. Mullins and R. F. Sekerka, J. Appl. Phys. **35**, 444 (1964).
[5]G. N. Young and S. H. Davis, Phys. Rev. B **34**, 3388 (1986).
[6]G. N. Young, S. H. Davis, and K. E. Brattkus (unpublished).
[7]A. Novick-Cohen (unpublished).
[8]R. A. Brown and L. H. Ungar, Phys. Rev. B **29**, 1367 (1984).
[9]R. A. Brown and L. H. Ungar, Phys. Rev. B **30**, 3993 (1984).
[10]R. A. Brown, M. J. Bennett, and R. A. Brown, Phys. Rev. B **31**, 5923 (1985).
[11]L. H. Ungar and R. A. Brown, Phys. Rev. B **31**, 5931 (1985).
[12]A. Novick-Cohen and G. I. Sivashinsky, Physica (The Hague) **20D**, 237 (1986).
[13]M. L. Frankel (unpublished).
[14]J. S. Langer, Rev. Mod. Phys. **52**, 1 (1980).
[15]J. M. Hyman, Los Alamos National Laboratory Report LA-7595-M, 1979 (unpublished).
[16]A. Novick-Cohen (unpublished)
[17]P. Rosenau, Phys. Lett. A **118**, 222 (1986).
[18]P. Rosenau, Phys. Rev. B **36**, 5868 (1987).